



Strength requirements for non-structural components responding nonlinearly under earthquake excitation

K. Haymes, R. Chandramohan & T.J. Sullivan

University of Canterbury, Christchurch.

ABSTRACT

This study develops a practice-oriented method to design non-structural components and their restraints to lower strengths than needed to remain elastic under earthquake ground motion by permitting nonlinear non-structural response. Non-structural design approaches based on elastic floor acceleration response spectra can be conservative for non-structural elements that are likely to respond nonlinearly under design level ground motions. Hence, this paper proposes a framework to design non-structural components to predicted inelastic floor response spectra instead.

The proposed framework for considering the nonlinear response of non-structural components builds upon a method recently developed by the authors to predict elastic floor response spectra using structural modal characteristics. The framework is developed and verified using floor motion records from instrumented buildings in New Zealand. The approach has been found to provide greater accuracy than current international non-structural design practices without compromising simplicity, to facilitate adoption in practical design applications. The motivation for developing this framework is to encourage the adoption of a more rational non-structural design philosophy, and thereby help limit seismic losses, which were shown in recent New Zealand earthquakes to be governed by damage to non-structural components. The findings also highlight the potential benefit of providing non-structural components with the ability to deform nonlinearly, either via inelastic behaviour or the provision of low-damage friction or rocking mechanisms.

1 INTRODUCTION

During an earthquake, the acceleration demands on non-structural components in a building tend to vary greatly from one level to another; hence, floor response spectra are required to help quantify design actions at different levels. A number of methods have been proposed to predict floor response spectra in the literature (e.g. Jiang et al. 2015; Kehoe & Hachem 2003; Vukobratović & Fajfar 2017; and Welch & Sullivan 2017). Kazantzi et al. (2020) proposed a method to predict strength-reduction factors that reduce floor response

spectra to account for non-structural nonlinearity. This paper develops a floor spectrum prediction method that expands upon the elastic floor acceleration response spectrum method proposed in Haymes et al. (2020), to make provisions for non-structural components responding nonlinearly while the supporting structure remains elastic. This provides the practitioner with a rational basis to design non-structural components and their restraints, that are likely to respond in the nonlinear range under design level ground motions, following a traditional force-based design framework. For well-detailed modern structures, the performance of non-structural components will likely govern the functionality of a building after an event, with many structural systems able to sustain little or no damage under moderate and high intensity shaking levels. Hence, the development of an inelastic floor spectrum prediction method for buildings responding elastically is considered to represent a valuable contribution to the state-of-the-art.

Direct estimation of floor response spectra permits the design seismic loading on non-structural components to be defined without requiring the computational effort associated with explicit modelling and time-history analysis of the non-structural component and the supporting structure. The framework developed in Haymes et al. (2020) considers non-structural components responding elastically by predicting floor spectral acceleration, $S_{FA}(T_{NS})$, given as the ratio of the seismic design force acting on a non-structural component, F_{NS} , and its weight, W_{NS} . Nonlinear non-structural response instead uses seismic design yield force $F_{y,NS}$, prescribed using the floor non-structural yield force coefficient, $C_{y,NS}$, given in Equation 1:

$$C_{y,NS} = \frac{F_{y,NS}}{W_{NS}} \quad (1)$$

Floor non-structural yield force coefficient response spectra are henceforth referred to as inelastic floor response spectra in this paper for brevity.

The work presented herein uses a total of 126 floor motion records from five instrumented buildings from the GeoNet Structural Array (GeoNet, 2021) as detailed in Haymes et al. (2020). Inelastic floor response spectra were computed from these records using INSPECT (Carr, 2016). The software computes inelastic floor response spectra by computing the response of SDOF oscillators with specified hysteretic properties for the input earthquake acceleration records and iterating to converge on a yield force required to obtain target displacement ductility values.

2 COMPARISON OF ELASTIC AND INELASTIC FLOOR RESPONSE SPECTRA

A key feature of floor acceleration response spectra is the dynamic amplification of demands where the period of the component is near one of the dominant modal periods of the supporting structure. An elastic floor response spectrum (corresponding to a non-structural displacement ductility μ_{NS} of 1.0 and non-structural damping ξ_{NS} of 2%) is plotted in Figure 1, computed from the transverse floor motion recorded at the roof of the University of Canterbury (UC) Physics building under the February 2011 earthquake. This illustrates the significant amplification above the peak floor acceleration (corresponding to a non-structural period T_{NS} of 0 s) at non-structural periods $0.45 \text{ s} < T_{NS} < 0.8 \text{ s}$ and $0.2 \text{ s} < T_{NS} < 0.4$, corresponding to the amplification associated with the fundamental and higher mode structural responses, respectively. Designing for the high demands observed in narrow period bands of elastic floor response spectra would require a significant increase in investment in strengthening. With uncertainties in predicting the damping of the non-structural component and the periods of vibration of both the non-structural component and the supporting structure, it is unlikely that a component will experience the peak amplification, particularly where the inelastic response of the building can lengthen the fundamental period of the structure.

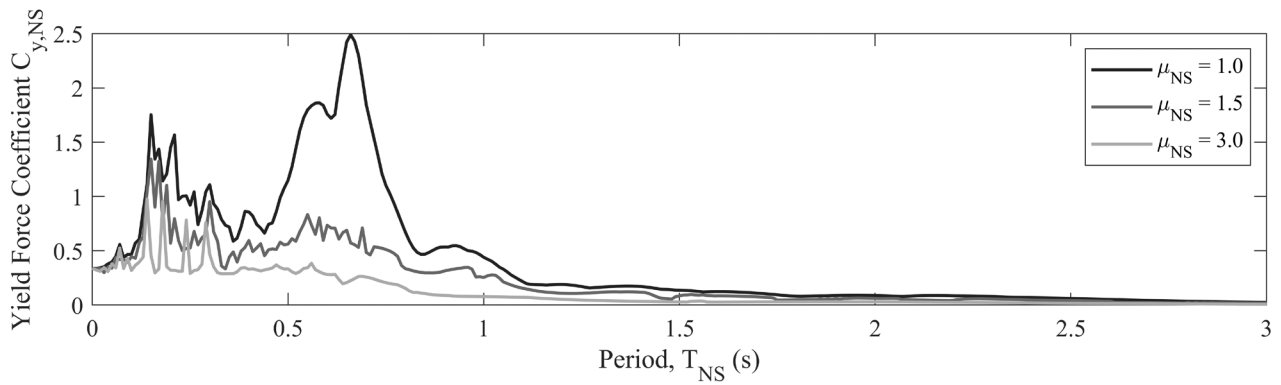


Figure 1: Floor response spectra computed using the February 2011 UC Physics building transverse roof record at non-structural damping $\xi_{NS} = 2\%$ for non-structural ductilities $\mu_{NS} = 1, 1.5, \text{ and } 3$.

In lieu of strengthening non-structural components to respond linearly, some types of non-structural components can instead be permitted to undergo nonlinear deformations. These deformations may be achieved through inelastic behaviour or by the provision of low-damage friction or rocking mechanisms. Nonlinear non-structural response is characterised using non-structural displacement ductility, μ_{NS} , as widely adopted in the literature (Kazantzi et al., 2020; Standards New Zealand, 2016). This enables the direct computation of the required non-structural strength as a function of the non-structural period, from an inelastic floor response spectrum. Figure 1 demonstrates the significant reduction in the yield force coefficient computed from the transverse floor motion recorded at the roof of the UC Physics building under the February 2011 earthquake motion by adopting non-structural ductilities μ_{NS} of 1.5 and 3.0.

3 OVERVIEW OF THE PREDICTION FRAMEWORK

The construction of the floor response spectrum using the proposed framework is illustrated in Figure 2. The framework uses the mode shapes and periods of the building to first compute the peak floor acceleration demands for each mode. Subsequently, dynamic amplification factors that depend on the damping ratio of the non-structural component and the ratio of the period of the non-structural component to each modal period of the supporting structure are used to establish the contributions of different modes to the total floor response spectrum. Finally, the predicted floor response spectrum is taken as the maximum spectral acceleration considering the acceleration response spectrum at the ground and the square-root-sum-of-squares (SRSS) of all of the modal contributions at each non-structural period.

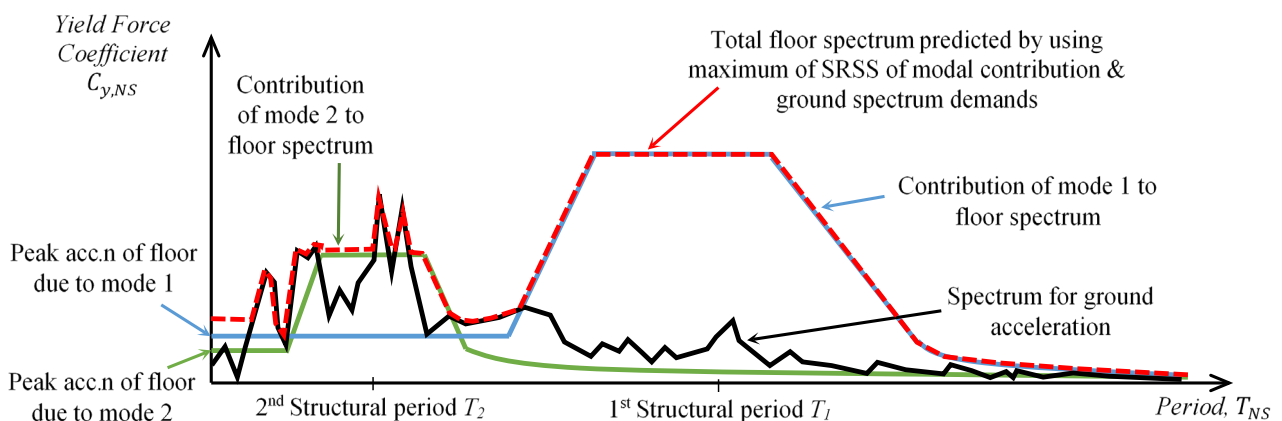


Figure 2: Overview of the elastic floor acceleration response spectrum prediction method from Haymes et al. (2020) showing modal contributions, ground response spectrum, and the SRSS combination approach.

The contribution of mode i at floor j to an inelastic floor response spectrum is computed using Equation 2:

$$C_{y,NS,i}(T_{NS}, \xi_{NS}) = \Gamma_i \Phi_{i,j} S_{GA}(T_i, \xi_{str}) DAF \quad (2)$$

where Γ_i is the participation factor of mode i ; $\Phi_{i,j}$ is the modal shape coordinate of mode i at floor j ; $S_{GA}(T_i, \xi_{str})$ is the ground acceleration response spectral ordinate corresponding to the period of vibration of mode i , T_i , scaled to the damping of the structure, ξ_{str} ; and DAF is the Dynamic Amplification Factor used to describe the amplification from the interaction between the fundamental mode of vibration of the non-structural element, T_{NS} , and mode of vibration i of the building, T_i .

The proposed DAF curves for elastic and inelastic non-structural responses are shown in Figure 3. Note that these are consistent, where the equations which provide for reductions due to non-structural inelasticity reduce to the elastic form when $\mu_{NS} = 1$. These curves are described by Equation 3:

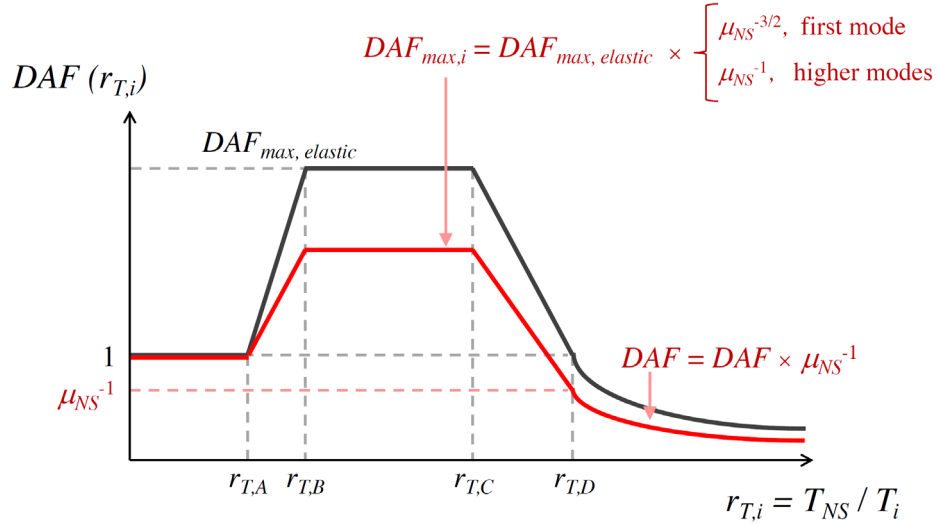


Figure 3: Dynamic amplification factor, DAF , including the provisions for non-structural inelasticity.

$$DAF = \begin{cases} 1 & r_{T,i} \leq r_{T,A} \\ \frac{r_{T,i} - r_{T,A}}{r_{T,B} - r_{T,A}} (DAF_{max,i} - 1) + 1 & r_{T,A} < r_{T,i} < r_{T,B} \\ DAF_{max,i} & r_{T,B} \leq r_{T,i} \leq r_{T,C} \\ \frac{r_{T,i} - r_{T,C}}{r_{T,D} - r_{T,C}} (1 - DAF_{max,i}) + DAF_{max,i} & r_{T,C} < r_{T,i} < r_{T,D} \\ \frac{1}{\mu_{NS}[(1 - r_{T,D}) + r_{T,C}]^2} & r_{T,D} \leq r_{T,i} \end{cases} \quad (3)$$

where $r_{T,A}$, $r_{T,B}$, $r_{T,C}$, and $r_{T,D}$ are specified period ratio values which determine the shape of the DAF curves (values of 0.6, 0.8, 1.2 and 1.6 are recommended, respectively), and DAF_{max} is the maximum dynamic amplification factor, given in Equation 4:

$$1 \leq DAF_{max} = [0.5\xi_{str} + \xi_{NS}]^{-2/3} \begin{cases} \mu_{NS}^{-3/2} & i = 1 \\ \mu_{NS}^{-1} & i > 1 \end{cases} \quad (4)$$

The inelastic floor response spectrum at the floor level j , for a non-structural component with a specified damping, ξ_{NS} , and ductility, μ_{NS} , given as $S_{FA,j}(T_{NS}, \xi_{NS})$, is defined by taking the maximum value of the modal contributions combined using square-root-sum-of-squares (SRSS) and the ground acceleration response spectrum as given by Equation 5:

$$C_{y,NS} = \max \left[\sqrt{\sum_i C_{y,NS,i}(T_{NS}, \xi_{NS}, \mu_{NS})^2}, C_{y,G}(T_{NS}, \xi_{NS}, \mu_{NS}) \right] \quad (5)$$

Where $C_{y,NS,j}(T_{NS}, \xi_{NS}, \mu_{NS})$ is the modal acceleration contribution of mode i , using the reduced dynamic amplification factors $DAF(r_{T,i}, \mu_{NS})$; and $C_{y,G}(T_{NS}, \xi_{NS}, \mu_{NS})$ is the ground response spectrum scaled to non-structural damping, ξ_{NS} , and ductility, μ_{NS} .

4 BASIS OF THE PREDICTION FRAMEWORK

The design yield force coefficient depends upon the period of non-structural component, T_{NS} ; non-structural ductility, μ_{NS} ; and the damping of the non-structural component, ξ_{NS} . These interactions can be observed by examining the ratio of elastic and inelastic floor response spectral ordinates, denoted as non-structural strength-reduction factor, $R(\mu_{NS})$, as stated in Equation 6:

$$R(\mu_{NS}) = \frac{S_{FA}(T_{NS}, \mu_{NS}=1)}{C_{y,NS}(T_{NS}, \mu_{NS})} \quad (6)$$

Where $C_{y,NS}(T_{NS}, \mu_{NS})$ is the yield force coefficient spectral ordinate at T_{NS} for a value of non-structural ductility, μ_{NS} ; and $S_{FA}(T_{NS}, \mu_{NS} = 1)$ is the corresponding elastic spectral ordinate.

Figure 4 shows median strength-reduction factors computed at all recorded levels in both recorded directions of the instrumented buildings. The strength-reduction factors were computed for $\xi_{NS} = 2\%$, 5% , and 10% for $\mu_{NS} = 3$, assuming elastic-perfectly-plastic hysteretic behaviour of the non-structural component. The behaviours observed in this figure provide the basis of the proposed prediction framework. These observations are supported by those in Kazantzi et al. (2020).

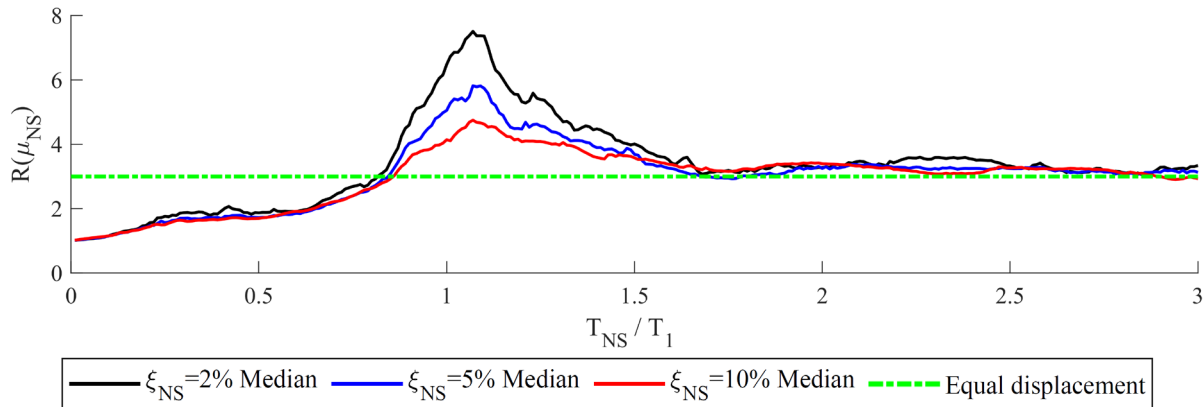


Figure 4: Median reduction factors using instrumented building records at all recorded floors. Spectra were computed at $\xi_{NS} = 2\%$, 5% , and 10% , at $\mu_{NS} = 3$.

4.1 Modal Contributions Considering Non-Structural Nonlinearity

The peak floor acceleration associated with each mode i is given by $\Gamma_i \Phi_{i,j} S_{GA}(T_i, \xi_{str})$. This quantity is unaffected by non-structural nonlinearity, as shown in Figure 4 where $R(\mu_{NS}, T_{NS} = 0) = 1$. Close observation of Equation 2 reveals that the most effective way to account for the influence of non-structural nonlinearity on the modal contributions is through modification of the DAF term.

Variation in the strength-reduction factors due to non-structural damping occurs in the period ranges $0.8 < T_{NS}/T_1 < 1.6$ and $0.3 < T_{NS}/T_1 < 0.5$, corresponding to the amplification associated with the fundamental and higher mode structural responses, respectively. In these regions, greater reductions are associated with lower non-structural damping ratios. The modified DAF_{max} term, given in Equation 4, considers the amplification

of spectral ordinates provided by decreasing non-structural damping, and the strength reduction provided by increasing non-structural ductility. The constant exponents in this equation vary for the fundamental and higher mode responses, with values $-3/2$ and -1 adopted, respectively, due to the observed differences in the corresponding strength-reduction factors. Although Figure 4 shows that significantly greater reductions are associated with the fundamental modal response than the higher modes, this is considered to be due to the dominance of the fundamental mode in most of the selected instrumented structures. Only the UC Physics building exhibited some substantive higher mode response, as shown in Figure 1. Floor motions recorded in this building were used to determine the power constant for higher modes. This has been further verified through comparison with inelastic floor response spectra from numerical modelling, which is outside of the scope of this paper.

The strength-reduction factors at $T_{NS}/T_1 > 1.6$ shown in Figure 4 are independent of non-structural damping and can be approximated by the equal displacement rule. This behaviour is described in the final line of the piecewise equation given in Equation 3.

4.2 Combination with Ground Response Spectra Considering Non-Structural Nonlinearity

The inelastic floor response spectrum is computed using Equation 6 by considering the maximum of the ground response spectrum and the SRSS of the modal contributions. This is based upon an empirical observation that some ordinates in floor response spectra are approximately unaltered from the corresponding ground response spectra, particularly at non-structural periods far longer than the fundamental structural period. It is thought that this behaviour is caused by rigid body motion of the structure, where non-structural components with these periods, mounted at any height in the building, have a similar peak responses to were mounted on the ground (refer also to Pozzi & Der Kiureghian (2012)).

The ground response spectrum must be scaled for both non-structural damping, as shown in Haymes et al. (2020), and non-structural ductility. Figure 5 shows floor and ground response spectra computed from the MBIE Stout St longitudinal floor 3 record at ξ_{NS} of 5% for non-structural ductilities μ_{NS} of 1, 1.5, and 3. The floor response spectrum approximates the corresponding ground ordinates for each value of non-structural ductility at non-structural periods greater than three times the structural fundamental period. Note that the y-axis of this plot uses a logarithmic scale to highlight the relatively low ordinates expected at these periods.

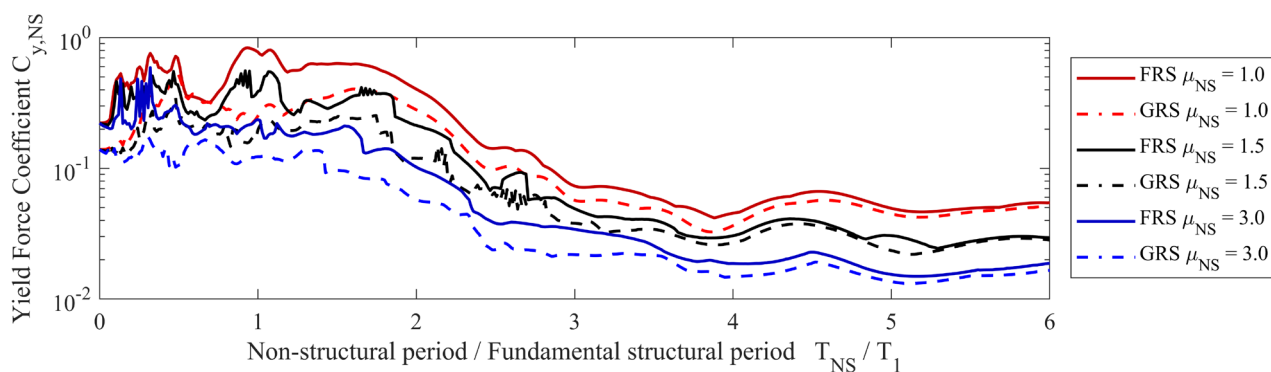


Figure 5: Floor (FRS) and ground (GRS) response spectra computed from the MBIE Stout St longitudinal floor 3 record. This is computed at $\xi_{NS} = 5\%$ for non-structural ductilities $\mu_{NS} = 1, 1.5, 3$.

NZS1170.5 provides a scaling factor, k_μ , to modify a design ground acceleration response spectrum for structural inelasticity (Standards New Zealand, 2016). This idea can be also be applied to account for non-structural inelasticity. The design ground acceleration response spectrum is modified by dividing the elastic spectrum by a reduction factor, k_μ . For soil classes A, B, C and D, k_μ is computed using Equation 7:

$$k_{\mu} = \begin{cases} \mu_{NS} & T_{NS} \leq 0.7 \text{ s} \\ \frac{(\mu_{NS}-1)T_{NS}}{0.7} & T_{NS} > 0.7 \text{ s} \end{cases} \quad (7)$$

5 COMPARISON OF THE PREDICTION FRAMEWORK

The performance of proposed framework and the NZS1170.5 provisions for non-structural nonlinearity are compared in Figure 6. Floor response spectra were computed for the UC Physics building Lyttelton 2011 transverse roof record for 5% non-structural damping and with non-structural ductilities of 1, 1.5, and 3.

The floor response spectrum prescribed by NZS1170.5 is independent of structural periods and assumes a spectral shape that is conservative at most ordinates and fails to predict the amplification of ordinates near resonance with the first and second structural modes in Figure 6(a) and (b), respectively. Conversely, the proposed framework is able to make more accurate predictions of the elastic amplification of ordinates around the structural periods and approximates the reduction with non-structural ductility well.

The peak floor acceleration (at $T_{NS} = 0$) is well predicted by the proposed framework. The spectral shape assumed by NZS1170.5 predicts a peak floor acceleration that is more than twice the observed elastic demand. The NZS1170.5 nonlinear non-structural reduction factors are period-independent, resulting in reductions of peak floor acceleration predictions which do not appear to have any physical basis.

Floor response spectral ordinates at $T_{NS} > 1$ s are significantly over-predicted by NZS1170.5. The adoption of the equal displacement rule for the modal contributions and the consideration of ground response spectra scaled to the corresponding non-structural ductility provide good approximations to the observed demand.

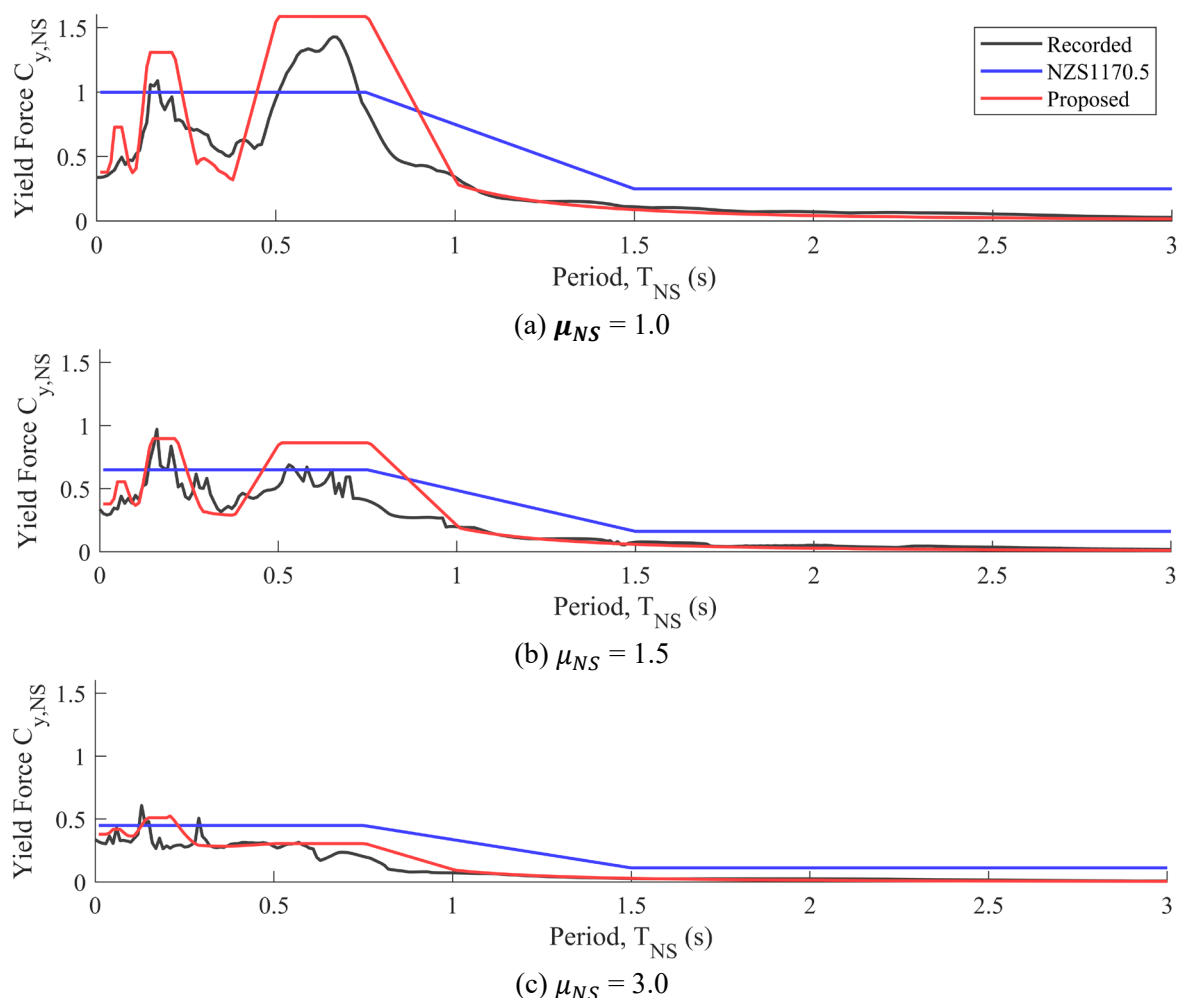


Figure 6: Recorded and predicted floor response spectra for the UC Physics building Lyttelton 2011 transverse roof record, at 5% non-structural component damping.

6 CONCLUSIONS

Seismic design of non-structural components for the demands prescribed through elastic floor response spectra could require significant strengthening due to the high-amplification of narrow-band floor spectrum ordinates associated with resonant behaviour between non-structural components and dominant modes of the supporting structures. If non-structural components can instead be permitted to undergo nonlinear deformation, strength requirements may be considerably reduced.

A robust framework to predict the required design yield strength was developed considering trends exhibited in inelastic floor response spectra. Recorded motions from instrumented building in New Zealand were used which demonstrated behaviours that may be expected in practice. The peak amplification of spectral ordinates near dominant structural modes increases for decreasing non-structural damping and reduces with increasing ductility. Provisions for these parameters were developed by considering the amplification associated with the structural fundamental and higher modal responses separately. Peak floor acceleration is independent of non-structural nonlinearity and was therefore unaltered from the elastic method. Demands at long non-structural periods were observed to be independent of non-structural damping and reductions were approximated using the equal displacement rule. Some ordinates in floor response spectra were observed to be approximately unaltered from the corresponding ground response spectra, possibly caused by rigid body motion of the structure. The predicted inelastic floor response spectrum therefore considers the maximum of the ground response spectrum scaled to non-structural damping and ductility and the modal contributions.

The proposed framework was compared with the current New Zealand standard provisions, NZS1170.5. The proposed approach outperformed the standard due to its stronger basis in physical behaviours. This illustrated that this method is well developed and able to be directly applied in engineering practice.

The findings highlight the potential benefit of providing non-structural components with the ability to deform nonlinearly, either via inelastic behaviour or the provision of low-damage friction or rocking mechanisms.

7 ACKNOWLEDGEMENTS

The use of the GeoNet structural array enabled the verification and refinement of the method presented in this paper. Thanks are given to GeoNet, the tenants and the owners of these buildings for the foresight in instrumenting these structures to provide such an excellent resource.

This project was (partially) supported by QuakeCoRE, a New Zealand Tertiary Education Commission-funded Centre. This is QuakeCoRE publication number 0648.

8 REFERENCES

- Carr, A. J. (2016). *INSPECT In-elastic Response Spectra Computation*. Carr Research Ltd.
- GeoNet. (2021). *Structural Array Data*. https://www.geonet.org.nz/data/types/structural_arrays
- Haymes, K., Sullivan, T., & Chandramohan, R. (2020). A practice-oriented method for estimating elastic floor response spectra. *Bulletin of the New Zealand Society for Earthquake Engineering*, 53(3), 116–136. <https://doi.org/10.5459/bnzsee.53.3.116-136>
- Jiang, W., Li, B., Xie, W.-C., & Pandey, M. D. (2015). Generate floor response spectra: Part 1. Direct spectra-to-spectra method. *Nuclear Engineering and Design*, 293, 525–546. <https://doi.org/10.1016/J.NUCENGDES.2015.05.034>
- Kazantzi, A. K., Miranda, E., & Vamvatsikos, D. (2020). Strength-reduction factors for the design of light nonstructural elements in buildings. *Earthquake Engineering & Structural Dynamics*, eqe.3292. <https://doi.org/10.1002/eqe.3292>
- Kehoe, B. E., & Hachem, M. (2003, January 1). Procedures for Estimating Floor Accelerations. *ATC-29-2 Seminar on Seismic Design, Performance, and Retrofit of Nonstructural Components in Critical Facilities*.
- Pozzi, M., & Der Kiureghian, A. (2012). Response spectrum analysis for floor acceleration. *15th World Conference on Earthquake Engineering*, 29906–29915.
- Standards New Zealand. (2016). *NZS 1170.5:2004: Structural design actions, Part 5: Earthquake actions - New Zealand*.
- Vukobratović, V., & Fajfar, P. (2017). Code-oriented floor acceleration spectra for building structures. *Bulletin of Earthquake Engineering*, 15(7), 3013–3026. <https://doi.org/10.1007/s10518-016-0076-4>
- Welch, D. P., & Sullivan, T. J. (2017). Illustrating a new possibility for the estimation of floor spectra in nonlinear multi-degree of freedom systems. *16th World Conference on Earthquake Engineering*.